EEET ECOLOGICAL ENGINEERING & ENVIRONMENTAL TECHNOLOGY

Ecological Engineering & Environmental Technology, 2026, 27(7), 15–31
https://doi.org/10.12912/27197050/221836
ISSN 2719–7050, License CC-BY 4.0

Received: 2026.05.03
Accepted: 2026.06.15
Published: 2026.07.01

Land cover change and carbon sequestration dynamics in a tropical karst landscape under secondary forest regeneration

Atma Wira Negara[1], Mukrimin[1,2*], Usman Arsyad[2], Hasanuddin[3], Sultan[3], Nilam Sari[4]

[1] Forestry Master Program, Faculty of Forestry, Hasanuddin University, 90245, Makassar, Indonesia
[2] Department of Forestry, Faculty of Forestry, Hasanuddin University, 90245, Makassar, Indonesia
[3] Forestry Study Program, Faculty of Agriculture, Muhammadiyah University of Makassar, Makassar, 90221, Indonesia
[4] Research Center for Ecology and Ethnobiology, National Research and Innovation Agency (BRIN), Jl. Raya Jakarta-Bogor Km. 46, Cibinong 16911, Indonesia
* Corresponding author's e-mail: mukrimin@unhas.ac.id

ABSTRACT

Karst ecosystems are often overlooked in national carbon calculations, despite having unique organic and inorganic carbon storage mechanisms. This study aims to analyze the dynamics of land cover and carbon storage capacity in the Bantimurung Sub-Watershed, Maros-Pangkep Karst Area, over a period of one decade (2014–2024). The research method uses the integration of multitemporal spatial analysis based on satellite imagery and high-level field measurements (Tier 3) according to the SNI 7724:2019 standard. The mapping results showed significant vegetation restoration, characterized by the expansion of secondary dryland forests of 229.48 ha, the majority of which came from open land conversion and mixed dryland agriculture. Terrestrial measurements revealed that these ecosystems hold an average carbon reserve of 177.89 tonnes C/ha, a value that has exceeded the national average for secondary forests and is equivalent to the quality of primary forests. In a span of ten years, the total carbon stocks in the study area increased by 29,909 tonnes C, proving the effectiveness of natural succession under the protected status of national parks. These findings confirm the importance of using site-specific carbon data as a technical basis in climate change mitigation planning and achieving Indonesia's FOLU Net Sink 2030 target in karst ecosystems.

Keywords: carbon stocks, karst ecosystems, secondary forests, land succession, Bantimurung sub-watershed.

INTRODUCTION

The increasing concentration of greenhouse gases, particularly carbon dioxide, driven by fossil fuel combustion, deforestation, and land-use change, represents a major driver of global climate change with far-reaching ecological, economic, and social consequences. Recent assessments indicate that continued anthropogenic emissions are reducing the Earth's capacity to maintain climatic stability (Friedlingstein et al., 2025; Forster et al., 2025). Within this context, the land use, land-use change, and forestry sector plays a dual role, acting both as a significant source of emissions under deforestation and as a major carbon sink through vegetation and soils (Friedlingstein et al., 2025).

Indonesia has strengthened its climate mitigation framework through the ratification of the Paris Agreement (2016, 2016) (and the implementation of carbon economic value policies (perpres 98, 2021) targeting the FOLU Net Sink 2030 goal. This national strategy positions forested landscapes as critical components in achieving net carbon absorption at the national scale.

Despite their importance, karst ecosystems remain underrepresented in carbon cycle studies and are often mischaracterized as

low-productivity landscapes. In contrast, karst systems exhibit unique carbon dynamics, storing both organic carbon in biomass and soils, and inorganic carbon through rock–water–CO_2 interactions driven by carbonate dissolution processes. Recent studies highlight that these coupled processes significantly contribute to global carbon cycling and cannot be neglected (Zhang et al., 2023; Zhou et al., 2023; Shi et al., 2025)

From a Karst Dynamic System (KDS) perspective, carbon cycling in karst landscapes is governed by tightly coupled interactions among the atmosphere, biosphere, hydrosphere, and lithosphere. This integrated system means that land cover change can significantly disrupt carbon fluxes, hydrological pathways, and the natural capacity of karst systems to function as carbon sinks (Shi et al., 2025). Consequently, degradation of vegetation cover produces a dual impact: loss of terrestrial biomass carbon and disruption of inorganic carbon sequestration mechanisms, which are unique to karst environments (Chen et al., 2020).

The Bantimurung sub-watershed, part of the Maros–Pangkep karst region in south Sulawesi, Indonesia, represents a highly relevant case study due to its ecological significance and increasing land-use pressure. Previous studies have shown that forest dynamics in this region are strongly associated with changes in carbon stocks, while the broader Maros karst system contains substantial carbon reserves and associated economic value (Fajri et al., 2024, 2025). However, rapid conversion of forested land into agricultural and cultivated systems continues to threaten ecosystem carbon storage capacity. Similar land-use transitions in tropical forests have been shown to result in substantial carbon losses across biomass and soil pools (Guillaume et al., n.d.) reinforcing concerns for karst regions undergoing similar pressures.

Secondary forest regeneration offers a potential pathway for restoring carbon sequestration functions in degraded tropical landscapes. Evidence from tropical forest systems indicates that regenerating secondary forests can accumulate significant carbon stocks and partially offset emissions from deforestation, with recovery of carbon storage closely linked to improvements in vegetation structure and ecosystem function (Rosa and Marques, 2022) However, the extent to which such recovery occurs in karst ecosystems, where hydrological and geochemical processes strongly interact with vegetation dynamics, remains poorly quantified.

A further limitation in existing carbon assessments is the widespread use of generalized default biomass values, which fail to capture spatial and ecological variability across forest types and successional stages. Tropical forest biomass is highly variable across ecological gradients, making site-specific assessments essential for improving carbon stock accuracy, particularly in structurally complex ecosystems such as karst landscapes (Rozendaal, 2022). In the Bantimurung sub-watershed, this need is amplified by shallow soil profiles, heterogeneous terrain, and highly variable regeneration stages.

Despite increasing attention to land-use change and carbon dynamics, a key knowledge gap remains: the lack of quantitative understanding of how multi-temporal land cover change influences carbon stock recovery during secondary forest regeneration in tropical karst systems. Previous studies have largely focused on geological or hydrological processes, with limited integration of spatial land-cover dynamics and empirically derived carbon stock changes across successional stages.

Therefore, this study aims to quantify the relationship between land cover change (2014–2024) and carbon stock dynamics in the Bantimurung Sub-Watershed karst ecosystem, integrating satellite-based land-use analysis with field-based biomass and soil carbon measurements. The study tests the hypothesis that secondary forest regeneration significantly enhances carbon sequestration capacity in karst landscapes, but that recovery rates vary spatially depending on land cover transition history and ecosystem condition. The expected outcome is a quantitative understanding of carbon recovery trajectories in tropical karst systems, providing improved parameterization for carbon accounting and supporting more accurate climate mitigation strategies in karst-dominated landscapes.

RESEARCH METHODS

Materials and methods

This study used a quantitative approach combined with spatial analysis to examine land cover change and carbon stock dynamics in the Bantimurung Sub-Watershed, South Sulawesi, Indonesia. The quantitative approach was used to calculate

land cover area, land cover transitions, and carbon stock estimates, while spatial analysis was used to examine the distribution and temporal pattern of land cover change during the 2014–2024 period. The research workflow included satellite image acquisition, image preparation, visual interpretation, manual on-screen digitizing, land cover accuracy assessment, carbon stock estimation, and analysis of historical carbon stock dynamics.

The study was conducted in the Bantimurung Sub-Watershed, Maros Regency, South Sulawesi Province, Indonesia. This area is part of the Maros–Pangkep karst landscape and is associated with the Bantimurung Bulusaraung National Park ecosystem. The location was selected because it represents a tropical karst landscape with high conservation value, varied topography, diverse land cover types, and a history of land cover change that is relevant to the analysis of carbon stock dynamics (Figure 1).

Types and data sources

This study used both primary and secondary data. Primary data were obtained through field observation, GPS-based land cover validation, vegetation biomass measurement in sample plots, litter sampling, and field documentation of land cover conditions. These data were used to support image interpretation, validate the land cover maps, and estimate site-specific carbon stock components.

Secondary data included satellite imagery, topographic data, climate data, watershed boundary data, and soil-related supporting information. Landsat 8 OLI/TIRS imagery was used to support land cover interpretation for the 2014 period, while Sentinel-2 imagery was used as the main satellite data source for land cover mapping in 2019 and 2024. Sentinel-2 imagery was obtained from Copernicus Browser and used to support visual interpretation and manual digitization. For the 2024 period, the analysis was strengthened by using high-resolution reference imagery at 1 meter per pixel. This reference imagery helped identify small forest patches, agricultural plots, settlement patterns, exposed karst surfaces, and secondary vegetation stages in greater detail.

Google Earth historical imagery was also used as supporting reference data, especially for interpreting historical land cover conditions in 2014 and 2019. In addition, the National Digital Elevation Model (DEMNAS) was used to describe the topographic characteristics of the study area. Daily rainfall data from NASA POWER for the 2014–2024 period were used as supporting environmental information, while soil type data from BBSDLP were used to describe the general biophysical condition of the karst landscape.

To maintain spatial and temporal consistency, all spatial datasets were processed using the same watershed boundary and coordinate reference system. The spatial data were projected into WGS 84 / UTM Zone 50S. Satellite images were clipped to the Bantimurung Sub-Watershed boundary and interpreted using the same land cover classification scheme. The resulting land cover maps were then used as the basis for land cover change analysis and historical carbon stock estimation.

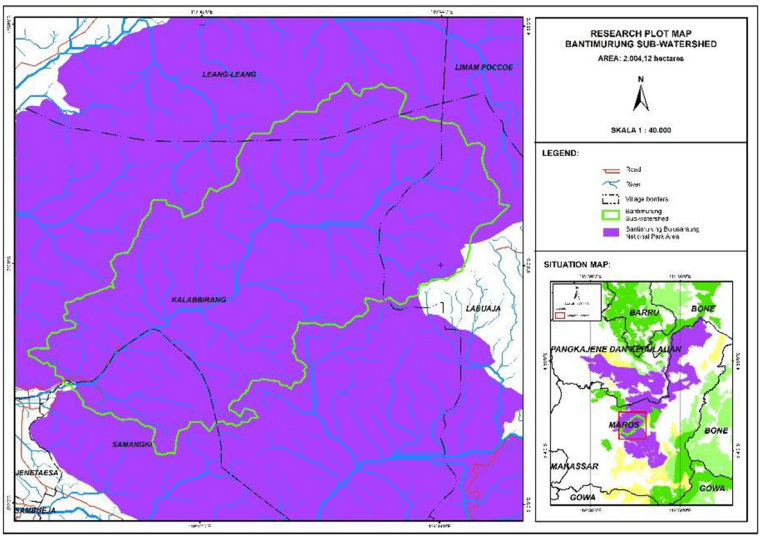

Figure 1. Map of the research location of the Bantimurung Sub Watershed, Kalabirang Village, Samangki Village, and Labuaja Village, Maros Regency

Data collection and analysis techniques

Land cover change analysis

Land cover change analysis was carried out using multi-temporal satellite imagery for 2014, 2019, and 2024. The analysis consisted of five main stages: satellite image acquisition, image preparation, visual interpretation, manual on-screen digitizing, and post-classification change detection.

Land cover mapping was conducted through visual interpretation and manual on-screen digitizing in ArcGIS Pro. Manual digitizing was used because the Bantimurung karst landscape contains mixed vegetation, exposed limestone surfaces, small agricultural plots, fragmented forest patches, and irregular land cover boundaries that are difficult to separate consistently using automatic classification. Therefore, algorithm-based classifiers such as Random Forest, Support Vector Machine, and Maximum Likelihood were not used. The term "supervised classification" in the previous version was revised to better reflect the actual mapping procedure used in this study.

Satellite imagery was selected based on image availability, low cloud disturbance, and visual clarity of land cover objects. Landsat 8 OLI/TIRS imagery was used to support interpretation for 2014, while Sentinel-2 imagery from Copernicus Browser was used for 2019 and 2024. Image visualization and interpretation were also supported by high-resolution reference imagery and, where applicable, enhanced Sentinel-2 outputs prepared through Google Colab with the S2DR3 workflow. The prepared images and reference data were then imported into ArcGIS Pro for manual on-screen digitizing.

For the 2024 land cover map, digitizing was conducted at a detailed working scale of 1:1,000. This scale was used to improve the delineation of small land cover features, including fragmented forest patches, settlement boundaries, agricultural plots, exposed karst surfaces, and secondary vegetation patches. The use of 1-meter high-resolution reference imagery supported more precise interpretation of land cover boundaries that are often less visible in medium-resolution imagery.

Visual interpretation was based on several interpretation keys, including tone or color, texture, shape, size, pattern, site condition, and association with surrounding landscape features. Primary dryland forest was identified by dense and continuous canopy cover, dark green tone, and coarse texture. Secondary dryland forest was identified by medium to dense vegetation cover, irregular canopy structure, and association with regenerating vegetation patches. Rice fields were recognized by regular plot patterns, smooth texture, and seasonal wet or dry appearance. Mixed dryland agriculture was identified by a mosaic pattern of crops, shrubs, and scattered trees. Open land was interpreted from bright tones and sparse or absent vegetation. Settlements were recognized from roof reflectance, clustered built-up structures, and road networks, while water bodies were identified by dark tone, smooth texture, and linear or pond-like forms.

The same land cover class definitions and interpretation criteria were applied to the 2014, 2019, and 2024 images to reduce interpretation bias and maintain comparability among observation years. After digitization, all polygons were checked for topology errors, boundary consistency, and attribute completeness before area calculation.

The land cover classes used in this study consisted of seven categories: primary dryland forest, secondary dryland forest, rice fields, mixed dryland agriculture, open land, settlements, and water bodies. After the land cover maps for 2014, 2019, and 2024 were completed, land cover change was analyzed using a post-classification comparison approach. The maps were overlaid to identify land cover transitions during the 2014–2019, 2019–2024, and 2014–2024 periods. The results were presented as land cover maps, area statistics, change detection maps, and land cover transition matrices to show the direction, magnitude, and spatial pattern of land cover transformation in the Bantimurung Sub-Watershed.

To improve reproducibility, screenshots of Copernicus Browser image selection, Google Colab/S2DR3 image preparation, ArcGIS Pro digitizing, spatial resolution checking, and final digitized land cover maps were prepared as supplementary materials

Land cover accuracy assessment

Accuracy assessment was conducted to evaluate the reliability of the land cover maps produced through visual interpretation and manual on-screen digitizing before the area data were used for carbon stock estimation. A total of 100 validation points were distributed across the mapped land cover classes using a stratified random sampling approach. This approach was used to ensure that all land cover classes were represented in the validation process. For the 2024 land cover map,

validation was conducted through field verification by comparing GPS-based reference points with the mapped land cover classes. For the 2014 and 2019 land cover maps, historical validation was supported by high-resolution Google Earth imagery, Copernicus imagery, and visual interpretation of stable landscape features. The validation data were then arranged in a confusion matrix to calculate Overall Accuracy, Producer's Accuracy, User's Accuracy, and the Kappa coefficient.

Overall Accuracy was used to measure the percentage of correctly mapped validation points from the total number of validation samples. Producer's Accuracy was used to evaluate how well reference land cover classes were represented on the map, while User's Accuracy was used to assess the probability that a mapped class actually corresponded to the same land cover condition in the reference data. The Kappa coefficient was used to measure the level of agreement between mapped land cover classes and reference data while accounting for agreement that may occur by chance.

Overall accuracy was calculated using the following formula:

$$OA = \frac{\sum x_{ii}}{N} \times 100\% \quad (1)$$

where: x_{ii} – the number of correctly mapped samples in the diagonal cells of the confusion matrix; N – the total number of validation samples.

Producer's accuracy (PA) was used to measure how well reference land cover classes were represented on the map, while user's accuracy (UA) was used to assess the probability that a mapped class actually corresponded to the same land cover condition in the reference data. The Kappa coefficient was used to measure the level of agreement between the mapped land cover classes and the reference data while accounting for agreement that may occur by chance. The Kappa coefficient was calculated using the following formula:

$$K = \frac{N\sum x_{ii} - \sum(x_{i+} \times x_{+i})}{N^2 - \sum(x_{i+} \times x_{+i})} \quad (2)$$

where: K – Kappa coefficient; N – total number of validation samples; x_{ii} – the number of correctly mapped samples in the diagonal cells of the confusion matrix; x_{i+} – row total; x_{+i} – column total.

A Kappa value greater than 0.80 was interpreted as strong agreement. Therefore, land cover maps with a Kappa value above this threshold were considered sufficiently reliable for land cover change analysis and subsequent carbon stock estimation

Carbon stock measurement

Carbon stock measurement was conducted to estimate the carbon storage capacity of forest land cover in the Bantimurung Sub-Watershed. The field measurement focused on two main forest land cover classes: primary dryland forest and secondary dryland forest. These classes were selected because they represent the main forest cover in the study area and are directly related to the assessment of secondary forest regeneration and carbon stock recovery.

Field sampling was carried out using a stratified purposive sampling approach. The sampling strata were determined based on the land cover maps derived from spatial analysis, with emphasis on primary dryland forest and secondary dryland forest. Plot locations were selected by considering land cover class, vegetation condition, accessibility, terrain condition, and representation of forest regeneration stages. A total of 27 plots were established across three sampling locations. These plots were distributed within primary dryland forest and secondary dryland forest areas to capture variation in vegetation structure and carbon stock conditions between mature forest stands and regenerating secondary forest stands.

The carbon stock assessment focused on three carbon components: aboveground vegetation biomass, litter, and soil organic carbon. Aboveground vegetation biomass and litter were measured directly from field data and calculation sheets, while soil organic carbon was included as a supporting component to describe belowground carbon contribution in the karst ecosystem. This component was interpreted carefully because karst landscapes commonly have shallow soil profiles, exposed limestone, rock fragments, and high spatial variability.

Aboveground biomass was measured in main plots measuring 20 × 20 m. In each plot, all trees and poles that met the measurement criteria were recorded and measured. Diameter at breast height (DBH) was measured at 1.3 m above the ground using a diameter tape. Tree height was also recorded because it was required in the biomass estimation equation. Tree species or local names were recorded where identification was possible. These field measurements were used as the basis

for estimating aboveground biomass. Aboveground biomass was estimated using the pantropical allometric equation developed by Chave et al. (2005), which uses wood density, diameter at breast height, and tree height as predictor variables. The equation is expressed as follows:

$$AGB = 0.0509 \times \rho \times D^2 \times H \quad (3)$$

where: AGB – aboveground biomass per tree (kg tree^{-1}); ρ – wood density (g cm^{-3}); D – diameter at breast height (cm); H – tree height (m).

In this study, a wood density value of 0.65 g cm^{-3} was used in the biomass calculation. The estimated biomass of each tree was then converted into carbon stock using a carbon fraction of 0.47, following forest carbon accounting guidelines and SNI 7724:2019. Aboveground biomass carbon was calculated using the following equation:

$$C_{AGB} = AGB \times 0.47 \quad (4)$$

where: C_{AGB} – aboveground biomass carbon stock; AGB – aboveground biomass; 0.47 – carbon conversion factor.

The carbon values obtained at plot level were then converted into tons C ha^{-1} based on the plot area. Since each main plot measured 20 × 20 m, or 400 m², plot-level carbon stock was converted to a hectare basis using the appropriate area conversion factor.

Litter carbon was measured from smaller subplots within the main vegetation plots. Litter materials found on the soil surface were collected and weighed to obtain fresh weight. Subsamples were then dried to obtain dry weight. The total dry weight of litter was estimated using the ratio between dry weight, wet weight, and total field weight. Litter biomass was then converted into carbon stock and expressed in tons C ha^{-1}. Litter was included because it represents an important transitional carbon pool between standing vegetation biomass and soil organic matter.

Soil organic carbon was calculated from soil carbon data available for the three sampling locations. The soil carbon calculation was based on organic carbon percentage values and converted into soil organic carbon stock per hectare. Because soil conditions in karst landscapes are highly heterogeneous, the soil organic carbon component was used to support the total carbon stock estimate and was interpreted with caution. Therefore, the main interpretation of carbon stock recovery in this study emphasized land cover change, aboveground biomass accumulation, and litter carbon.

The total carbon stock was calculated by combining vegetation carbon, litter carbon, and soil organic carbon using the following equation:

$$C_{total} = C_{AGB} + C_{litter} + C_{SOC} \quad (5)$$

where: C_{total} – total carbon stock; C_{AGB} – aboveground biomass carbon; C_{litter} – litter carbon; C_{SOC} – soil organic carbon.

All carbon stock values were expressed in tons C ha^{-1}. The average carbon stock value from the three sampling locations was then used as the forest carbon stock factor for estimating historical carbon stock dynamics. Detailed results of vegetation carbon, litter carbon, soil organic carbon, and total carbon stock are presented in the Results section.

Analysis of historical carbon stock dynamics

Historical carbon stock dynamics were analyzed using a stock-difference approach based on the IPCC carbon accounting framework. This approach estimates changes in carbon stock by comparing carbon stocks between observation years using land cover area and carbon stock factors.

In this study, land cover maps for 2014, 2019, and 2024 were used as activity data. Forest cover consisted of primary dryland forest and secondary dryland forest. The forest cover area for each observation year was obtained from the manually digitized land cover maps. The carbon stock factor was derived from the field-based carbon stock calculation from 27 plots distributed across three sampling locations representing primary dryland forest and secondary dryland forest.

The estimated forest carbon stock for each observation year was calculated using the following equation:

$$C_{year} = A_{forest} \times CF_{forest} \quad (6)$$

where: C_{year} is the estimated forest carbon stock for a given year, A_{forest} is the forest cover area derived from the land cover map, and CF_{forest} is the forest carbon stock factor obtained from field measurement.

Carbon stock change between periods was calculated using the following equation:

$$\Delta C = C_{t2} - C_{t1} \quad (7)$$

where: ΔC is the change in carbon stock, C_{t2} is the carbon stock in the later year, and C_{t1} is the carbon stock in the earlier year.

Because field carbon measurements were conducted under the current forest condition, historical carbon stock estimates for 2014 and 2019 were interpreted as estimates based on land cover change and the available field-derived carbon stock factor. This approach was used to evaluate the effect of forest cover dynamics, particularly the expansion of secondary dryland forest, on carbon stock recovery during the 2014–2024 period. The uncertainty related to temporal variation in carbon density was acknowledged because vegetation structure and carbon density in earlier years may not have been identical to the current field condition.

To reduce overestimation, the historical carbon stock analysis focused on forest cover classes, particularly primary dryland forest and secondary dryland forest. Non-forest land cover classes, such as settlements, open land, water bodies, rice fields, and mixed dryland agriculture, were not emphasized in the main carbon stock recovery analysis because their carbon stocks are generally lower, more variable, and strongly influenced by land management practices and seasonal cycles.

The results of the historical carbon stock analysis were presented as forest cover area, estimated carbon stock, carbon stock change between periods, and the contribution of secondary forest regeneration to carbon stock recovery in the Bantimurung karst landscape (Figure 2).

Figure 2. Field data collection activities for evaluating carbon sequestration dynamics under secondary forest regeneration: (a–b) measurement of tree diameter for aboveground biomass and carbon stock estimation; (c) establishment and observation of vegetation plots to assess stand structure and species composition; (d) soil sample collection; (e) collection and labeling of soil samples at 0–30 cm depth; and (f) assessment of understory vegetation and natural regeneration

RESULTS AND DISCUSSION

Land cover

Land cover change in the Bantimurung Sub-Watershed

The land cover analysis showed clear spatial and temporal changes in the Bantimurung Sub-Watershed during the 2014–2024 period. The most important pattern was the substantial increase in secondary dryland forest, accompanied by a sharp decline in open land and mixed dryland agriculture. These changes indicate a transition from open or intensively used land toward more vegetated land cover, particularly secondary forest regeneration. Changes in Land Cover in the Bantimurung Sub-Basin are as follows (Table 1).

The mapping results showed that the area of Primary Dryland Forests at the research site tended to be stable despite slight fluctuations. In 2014, the identified area was 1,698.77 ha (84.76%), rising to 1,773.88 ha (88.51%) in 2019, before finally correcting slightly to 1,686.49 ha (84.14%) in 2024. Although there was no massive degradation, the downward trend in the last period signaled the urgency of land conversion that began to affect the cover structure in the study area. The most contrasting phenomenon can be seen in the drastic expansion of Secondary Dryland Forests; from only 2.9 ha (0.14%) in 2014, to 79.53 ha (3.97%) in 2019, to reach 232.38 ha (11.59%) in 2024. Spatial tracing revealed that the majority of the increase in secondary forest area came from the conversion of mixed dryland and open land agriculture. The transformation reflects the shift from intensive land use to a more established vegetation phase. This condition indicates that vegetation restoration does not occur by chance, but is the result of the natural regeneration process as well as the effectiveness of land rehabilitation policies and improved resource governance. This pattern reinforces the findings of previous research that affirm that policy interventions and restoration schemes play a crucial role in driving the transition to natural vegetation ((Valencia et al., 2024) (Krause et al., 2016) (Robin et al., 2020)

The area of open land recorded a very sharp decline throughout the observation period. It was recorded that in 2014, open land was still 123.56 ha (6.17%), but this figure shrank drastically to only 0.40 ha (0.02%) in 2019, and continues to decrease until there is 0.20 ha (0.01%) left in 2024. This massive decline indicates that almost all open areas have undergone a significant functional transformation. Based on the matrix of land cover change, most of these areas are converted into secondary dryland forests and rice fields. The phenomenon is likely influenced by technical factors at the time of image recording; Areas that in the initial period have not been used or have just been opened, in the next period they have been processed into productive land or covered with natural vegetation. Most of these open lands also show indications of spontaneous vegetation recovery which was later identified as secondary forest. The pattern of transition from open land to more productive or vegetation-covered uses is in line with the findings, which relate the phenomenon to the dynamics of land management and socio-economic changes in the region.

Table 1. Bantimurung sub watershed land cover for the 2014, 2019, and 2024 periods

No.	Land cover	2014				2019		Remarks		2024	
		Area (Ha)	Percentage (%)	Remarks		Area (Ha)	Percentage (%)			Area (Ha)	Percentage (%)
1	Primary dryland forests	1698.77	84.76	75.11	15.02	1773.88	88.51	-87.71	-17.54	1686.17	84.14
2	Secondary dryland forest	2.90	0.14	76.63	15.33	79.53	3.97	152.85	30.57	232.38	11.59
3	Open land	123.56	6.17	-123.16	-24.63	0.40	0.02	-0.20	-0.04	0.20	0.01
4	Settlements	9.48	0.47	-4.66	-0.93	4.82	0.24	0.12	0.02	4.94	0.25
5	Mixed dryland agriculture	149.65	7.47	-33.91	-6.78	115.74	5.78	-112.14	-22.43	3.60	0.18
6	Rice fields	18.53	0.92	8.46	1.69	26.99	1.35	46.53	9.31	73.52	3.67
7	Water body	1.24	0.06	1.52	0.30	2.76	0.14	0.56	0.11	3.32	0.17
Total area		2004.13	100.00			2004.12	100.00			2004.12	100.00

Residential land cover shows a tendency to decrease in area during the observation period. In 2014, the residential area was recorded at 9.48 ha (0.47%), then decreased to 4.82 ha (0.24%) in 2019, and was relatively stable with a slight increase to 4.94 ha (0.25%) in 2024. Despite small fluctuations, the proportion of settlements to the total area remains low. Tracking changes between land cover classes shows that the decline in about ±5 ha of residential area since 2014 has mostly shifted to water bodies, secondary dryland forests, and road or open land networks. In 2019, some residential areas remain as residential areas, while others are transformed into mixed dryland farms. Furthermore, in 2024, the area that was previously residential and mixed dryland agriculture will develop into mixed dryland agriculture, rice paddies, and secondary dryland forests.

A drastic decline occurred in the mixed dryland agriculture sector throughout the observation period. From an area of 149.65 ha (7.47%) in 2014, this figure shrank to 115.74 ha (5.78%) in 2019, and declined sharply until only 3.60 ha (0.18%) remained in 2024. The land use conversion matrix revealed that in the 2014–2019 period, this reduction was driven by conversion to primary and secondary dryland forests. This trend continues in 2019–2024, where the rest of the agricultural land is transformed into secondary forests and rice fields. This shift reflects the transition from traditional dryland systems to more established vegetation cover as well as the intensification of agriculture through the expansion of rice fields.

In line with this phenomenon, rice field cover shows consistent growth: from 18.53 ha (0.92%) in 2014, increasing to 26.99 ha (1.35%) in 2019, and jumping to 73.52 ha (3.67%) in 2024. Spatial analysis confirmed that in the early period, rice fields developed from mixed dryland agriculture, while in the second period, much of the growth came from secondary dryland forests. This phenomenon indicates a shift in the socio-economic pattern of the community towards a more intensive and managed rice farming system. Economic factors, such as low productivity of dryland agriculture compared to the potential for higher and more stable rice fields, are the main driving forces of this transition.

In karst areas with challenging soil contours, shifting farming patterns used to be a survival strategy to maintain soil fertility cycles (Bennett et al., 2020). However, the increasing demands of food security encourage farmers to switch to a rice field system whose results are more predictable and controlled, especially with the support of irrigation technology (Ii et al., 2021) These changes are in line with the findings (Chen et al., 2020) emphasizing that the land management strategy will always adapt to economic efficiency and resource availability. Finally, the water body component also recorded a slight but steady increase trend, from 1.24 ha (0.06%) in 2014 to 3.316 ha (0.17%) in 2024.

Overall, the change in land cover in the study area shows the dynamics of land use that occur gradually and are interrelated between cover classes. Primary dryland forests tend to be stable with relatively small changes in area; this condition reflects that forest areas are still able to maintain their existence despite still experiencing conversion pressure on a limited scale. Similar patterns have been widely reported in recent studies showing that changes in primary forests generally occur slowly and are not always followed by a large loss of area (Curtis et al., 2018) (Donchyts et al., 2022).

On the other hand, the increase in secondary dryland forests indicates the ongoing process of real land restoration. The growth of this cover class is generally related to natural regeneration and land rehabilitation programs carried out after reduced agricultural activities or intensive land use. These findings are in line with the results of the study (Robin et al., 2020) and (Meyfroidt et al., 2022) which confirms that the increase in secondary forests is often the main feature of landscape transitions in areas that have experienced changes in land management policies and socio-economic dynamics.

The significant decline in open land and mixed dryland agriculture, along with an increase in rice paddies, indicates a shift in the land use system towards a more managed and productive form. This pattern is widely found in recent studies that explain that dryland agriculture tends to be abandoned due to its low productivity, while rice field systems are chosen because they are more stable and have higher yield certainty (Meyfroidt et al., 2022)(Shamim et al., 2020). This condition reflects the community's efforts to adjust the land management strategy to the needs of food security and production efficiency.

The change in the relatively small area of the settlement and the increase in the water body indicate an adjustment of spatial function that is local and non-dominant, but still contributes to changes in the overall landscape structure. This pattern

is in line with recent research findings that land cover changes in many areas are driven more by changes in agricultural practices and vegetation restoration than by the expansion of built-up areas (Patterns et al., 2021) (Meyfroidt et al., 2022). In general, the results of this study show that land cover change in the study area is an adaptive process influenced by the interaction between environmental conditions, human activities, and land management policies, with a tendency towards landscapes that are more covered by vegetation and more managed in the long term.

Land cover accuracy assessment

The reliability of the land cover map was evaluated using 100 validation points distributed across the mapped land cover classes. The validation was conducted to ensure that the land cover data used for carbon stock estimation were sufficiently reliable. For the 2024 map, validation was supported by field verification and GPS-based reference points. For the 2014 and 2019 maps, historical validation was supported by Google Earth historical imagery, Copernicus imagery, and stable landscape features (Table 2).

The accuracy assessment showed that the manually digitized land cover map had an Overall Accuracy of 89% and a Kappa coefficient of 0.845. These values indicate strong agreement between the mapped land cover classes and the reference data. The primary dryland forest class showed the highest reliability, with a Producer's Accuracy of 95.4% and a User's Accuracy of 93.3%. The secondary dryland forest class also showed acceptable accuracy, with both Producer's Accuracy and User's Accuracy values of 84.0%. These results indicate that the manual on-screen digitizing approach provided a reliable spatial basis for analyzing forest regeneration and estimating carbon stock dynamics in the Bantimurung Sub-Watershed. However, the dryland agriculture class showed a lower Producer's Accuracy of 62.5%, indicating some confusion with other land cover classes, particularly rice fields and secondary vegetation. Therefore, land cover transitions involving agricultural classes were interpreted with caution.

The validation point distribution, GPS records, field photographs, Google Earth reference images, digitized land cover polygons, and the full confusion matrix are provided as supplementary materials to support the reliability of the land cover mapping results.

The confusion matrix shows that the forest land cover classes had a high level of mapping reliability. Primary dryland forest obtained a Producer's Accuracy of 95.4% and a User's Accuracy of 93.3%, while secondary dryland forest obtained both Producer's Accuracy and User's Accuracy values of 84.0%. These values indicate that the mapped forest classes were generally consistent with the reference data and can be used as a reliable spatial basis for analyzing forest regeneration and carbon stock dynamics.

Overall Accuracy was calculated from the diagonal values of the confusion matrix as follows:

$$OA = \frac{42+21+10+5+6+5}{100} \times 100 = 89\% \quad (8)$$

The Kappa coefficient was calculated based on the agreement between the mapped land cover classes and the reference data while accounting for agreement that may occur by chance. Based on the confusion matrix, the Kappa coefficient was obtained as follows:

Table 2. Confusion Matrix land cover mapping

Field validation / interpretation results	Primary dryland forests	Secondary dryland forest	Rice fields	Dryland agriculture	Settlements	Water body	Total	User's accuracy
Primary dryland forests	42	3	0	0	0	0	45	93.3%
Secondary dryland forest	2	21	1	1	0	0	25	84.0%
Rice fields	0	1	10	1	0	0	12	83.3%
Dryland agriculture	0	0	1	5	0	0	6	83.3%
Settlements	0	0	0	1	6	0	7	85.7%
Water body	0	0	0	0	0	5	5	100%
Total	44	25	12	8	6	5	100	
Producer accuracy	95.4%	84.0%	83.3%	62.5%	100%	100%	95.4%	

$$K = \frac{(100\times89)-2.864}{10.000-2.864} = 0.845 \quad (9)$$

An Overall Accuracy of 89% indicates that the manually digitized land cover map had a high level of accuracy. The Kappa coefficient of 0.845 also indicates strong agreement between the mapped land cover classes and the reference data. However, the dryland agriculture class showed a lower Producer's Accuracy of 62.5%, indicating some confusion with other land cover classes, particularly rice fields and secondary vegetation. Therefore, land cover transitions involving agricultural classes were interpreted with caution.

Carbon stock in 2024

Carbon stock calculation was conducted to evaluate the carbon storage capacity of forest land cover in the Bantimurung Sub-Watershed. The calculation was based on field data collected from sampling plots representing primary dryland forest and secondary dryland forest. Following SNI 7724:2019, three carbon components were considered in this study: aboveground vegetation biomass, litter, and soil organic carbon (Nasional and Nasional, 2019).

Aboveground vegetation biomass consisted of tree and pole biomass. Litter represented organic material found on the forest floor that had not fully decomposed, while soil organic carbon represented carbon stored in the soil component. The combination of these three components was used to estimate the total carbon stock of the forest ecosystem in the study area.

Vegetation carbon stock

The aboveground vegetation biomass component was the main contributor to carbon storage in the Bantimurung Sub-Watershed. Tree-level vegetation contributed a larger proportion of carbon stock than pole-level vegetation. The carbon stock from tree-level vegetation is presented in Table 3, while the carbon stock from pole-level vegetation is presented in Table 4.

The aboveground vegetation biomass component, consisting of tree and pole levels, was the main contributor to carbon storage in the Bantimurung Sub-Watershed, with an average value of 146.27 tons C ha^{-1}. This value indicates that forest stands in the study area have relatively high biomass accumulation, particularly in areas with larger tree diameters, denser canopy cover, and more developed stand structure. These structural characteristics suggest that several forest patches in the Bantimurung karst landscape are able to maintain substantial aboveground carbon storage.

The presence of large-diameter trees has important implications for carbon dynamics because larger trees generally store greater amounts of biomass and carbon than smaller or younger individuals. Forest stands with more developed canopy structure also tend to support higher carbon accumulation compared with more open or recently disturbed vegetation. Therefore, the relatively high vegetation carbon stock observed in this study indicates the important role of forest structure in maintaining carbon storage capacity in the Bantimurung Sub-Watershed.

The carbon storage capacity of the study area is also related to the biophysical characteristics of the karst ecosystem. Although karst landscapes are often associated with shallow and rocky soils, protected karst forests can still support substantial biomass accumulation when vegetation cover is maintained. This finding is consistent with (Fajri et al., 2024) who emphasized that tropical karst ecosystems should not simply be regarded as marginal landscapes with low productivity. In the Bantimurung Sub-Watershed, the combination of forest cover, karst terrain, and relatively mature stand structure appears to support aboveground carbon storage. Therefore, maintaining karst forest conservation areas is important for supporting ecosystem-based climate change mitigation

Table 3. Carbon content of vegetation tree level

No.	Biomass {Slopes)	Recommendation/Content C	Recommendation/Content C	Recommendation/Content C
	(kg/tree)	(kg/tree)	(kg/plot)	(kg/ha)
1	2478.009	1164.664	2.912	72.792
2	2980.784	1400.969	3.502	237.664
3	3926.659	1845.530	4.614	115.346
Total				425.801
Average				141.934

Table 4. Carbon content of pole level vegetation

No.	Biomass (kg/tree)	Recommendation/Content C (kg/tree)	Recommendation/Content C (kg/plot)	Recommendation/Content C (kg/ha)
1	23.61	11.10	0.11	11.10
2	0.00	0.00	0.00	0.00
3	64.62	30.37	0.08	1.90
Total				13.00
Average				4.33

Carbon litter stock

The contribution of litter carbon in the Bantimurung Sub-Watershed was relatively small compared with aboveground vegetation biomass, with an average value of 2.39 tons C ha^{-1}. The measured litter carbon stock ranged from 1.62 to 3.71 tons C ha^{-1} across the observation plots. This variation indicates differences in litter input, vegetation structure, canopy condition, and decomposition processes among plots. Although litter contributed less to the total carbon stock than tree biomass, it remains an important component in forest carbon and nutrient cycling. Litter represents organic material that is continuously deposited on the forest floor and acts as a transitional carbon pool between standing vegetation and soil organic matter. Through decomposition by microorganisms and soil fauna, litter material is gradually transformed into more stable organic matter and contributes to soil organic carbon formation.

The decomposition process is influenced by litter quality, litter quantity, temperature, humidity, understory vegetation, and local environmental conditions. These factors are particularly important in karst forest ecosystems, where soil depth, rock fragments, and microclimatic variation may affect the rate of organic matter decomposition and soil carbon accumulation. Therefore, although the litter carbon stock was quantitatively lower than vegetation biomass, litter plays an important role in maintaining soil carbon input and supporting ecosystem nutrient cycling. The results in Table 5 show that litter carbon stock varied among plots, with the highest value recorded in Plot 3 and the lowest value recorded in Plot 5. This variation suggests that litter accumulation and decomposition conditions were not uniform across the sampling area. Similar findings have been reported by (Wu et al., 2025) who showed that litter quantity and microclimatic conditions influence soil carbon dynamics. (Gautam and Berg, 2025) also emphasized that decomposition processes are important for maintaining forest ecosystem function and soil carbon stability.

For the total carbon stock calculation, the plot-level litter values were aggregated according

Table 5. Carbon content of litter

No.	Plot	Total weight	Wet weight (gr)	Dry weight (gr)	Total dry weight/Plot (g)	Biomass (g)	C in g/ha	C in kg/ha	tons/ ha
1	Plot 1	335	198.5	64.97	109.65	54.82	2192942.07	2192.94	2.19
2	Plot 2	370	182.9	71.61	144.86	72.43	2897288.14	2897.29	2.90
3	Plot 3	490	192.7	72.97	185.55	92.77	3710980.80	3710.98	3.71
4	Plot 4	340	214.3	68.19	108.19	54.09	2163751.75	2163.75	2.16
5	Plot 5	328	181.8	45.02	81.22	40.61	1624484.05	1624.48	1.62
6	Plot 6	335	182	49.64	91.37	45.69	1827406.59	1827.41	1.83
7	Plot 7	370	295.2	76.47	95.85	47.92	1916930.89	1916.93	1.92
8	Plot 8	490	210.9	66.77	155.13	77.57	3102636.32	3102.64	3.10
9	Plot 9	340	162.1	61.17	128.30	64.15	2566045.65	2566.05	2.57
10	plot 10	328	213.3	60.82	93.53	46.76	1870507.27	1870.51	1.87
Total									23.87
Average									2.39

to their corresponding sampling locations before being combined with vegetation carbon and soil organic carbon. Therefore, the average litter value presented in this section represents plot-level litter carbon, while the site-level litter values are presented in the total carbon stock table.

Litter plays an important role in linking carbon stored in vegetation with carbon stored in the soil. As plant residues accumulate on the forest floor, they become an important source of organic matter for soil carbon formation. Through decomposition by microbial communities and soil fauna, coarse litter materials are gradually transformed into more stable forms of organic matter that contribute to soil organic carbon (SOC).

Although its contribution to total carbon stock is smaller than that of tree biomass, litter remains important for maintaining soil carbon input and nutrient cycling in forest ecosystems. In the Bantimurung karst landscape, this role is particularly relevant because soil conditions are generally shallow, rocky, and spatially variable. Therefore, litter contributes not only to carbon storage, but also to the maintenance of soil organic matter and ecosystem functioning. This interpretation is in line with Gautam and Berg (2025), who emphasized the important role of decomposition processes in supporting forest ecosystem stability.

Soil carbon stock

Based on the analysis, the average soil organic carbon (SOC) stock in the Bantimurung Sub-Watershed was 23.67 tons C ha^{-1}. This value suggests that soil contributes to the overall carbon stock of the Bantimurung karst landscape. In karst ecosystems, soil carbon may accumulate in shallow soil layers and in microhabitats associated with epikarst structures. These conditions can support the retention of organic matter, particularly when vegetation cover is maintained and soil disturbance remains limited.

However, the SOC result should be interpreted with caution because karst soils are generally shallow, rocky, and spatially heterogeneous. According to Brown (2002), thin karst soils have limited buffering capacity against external disturbances. Land clearing, vegetation removal, or tree cutting can accelerate organic matter oxidation and increase the risk of carbon loss from the soil surface. Therefore, the protection of vegetation cover is important not only for maintaining aboveground biomass carbon, but also for supporting soil organic carbon stability in the Bantimurung karst ecosystem (Table 6).

This interpretation is supported by (Zhang et al., 2023) (Liu et al., 2023) who reported that land conversion in tropical karst ecosystems can increase soil respiration and accelerate the loss of organic carbon, particularly in the surface soil layer. (Liu et al., 2023) further suggested that when vegetation cover is disturbed, karst soils that function as carbon sinks may become potential carbon sources due to increased organic matter decomposition and carbon release. Therefore, although the SOC value in the Bantimurung Sub-Watershed indicates a contribution to belowground carbon storage, its long-term stability depends strongly on the maintenance of forest cover and the reduction of land disturbance.

Estimated average carbon stock

The carbon stock analysis showed that the forest ecosystem in the Bantimurung Sub-Watershed has a substantial carbon storage capacity. Based on field measurements and carbon stock calculations, the average total carbon stock in 2024 was estimated at 177.89 tons C ha^{-1}.

This value was estimated using a field-based approach consistent with Tier 3 principles, particularly for the vegetation and litter components. The calculation combined three carbon components: aboveground vegetation biomass, litter, and soil organic carbon. Vegetation biomass and litter were derived from field measurement data, while soil organic carbon was included as a supporting component to represent belowground

Table 6. Soil carbon content

Site	%C	SOM/Plot	SOM/ha	SOC/Ha
Site 1	1.6	2.7584	27.584	16.0
Site 2	3	5.172	51.72	30.0
Site 3	2.5	4.31	43.1	25.0
Total				71.0
Average				23.67

carbon storage in the karst ecosystem. The calculation referred to SNI 7724:2019 and relevant IPCC carbon accounting guidelines to ensure that the estimated carbon stock reflected site-specific conditions in the Bantimurung Sub-Watershed.

The average carbon stock value of 177.89 tons C ha^{-1} was then used as a site-specific forest carbon stock factor for estimating historical carbon stock dynamics during the 2014–2024 period. This approach provides a more localized estimate than the use of general default values, although the results should still be interpreted with consideration of spatial variation in vegetation structure, litter accumulation, and soil organic carbon conditions (Table 7).

The measurement results showed that the average total carbon stock in the Bantimurung Sub-Watershed reached 177.89 tons C ha^{-1}. This value indicates that the forest ecosystem in the study area has a relatively high carbon storage capacity. When compared with the 2022 Indonesia Forest Reference Level document, this value is within the range of national forest carbon reference values and is close to the reported value for primary forest carbon stock. However, this comparison should be interpreted carefully because carbon stock estimates may differ depending on the carbon pools included, the measurement approach, and site-specific ecological conditions.

The relatively high carbon stock in the Bantimurung Sub-Watershed is likely influenced by the biophysical characteristics of the Maros–Pangkep karst ecosystem, particularly forest structure, vegetation density, and the accumulation of organic matter. These findings are consistent with Yudono et al. (2022), who reported that canopy structure and forest stand complexity in protected forest areas of South Sulawesi contribute to maintaining carbon stocks above 150 tons C ha^{-1}. In this study, the dominance of aboveground vegetation biomass indicates that forest structure plays an important role in supporting carbon storage in the Bantimurung karst landscape. The use of site-specific field data provides an advantage over the use of general default values because it better reflects local ecological conditions. In this study, vegetation biomass and litter were estimated using field-based measurements, while soil organic carbon was included as a supporting component of total carbon stock. This approach helps reduce uncertainty in local carbon stock estimation and provides a more realistic basis for climate mitigation planning, carbon accounting, and sustainable watershed management in karst-dominated landscapes.

Historical carbon stock dynamics (2014–2024)

Analysis of historical carbon stock dynamics was conducted to evaluate changes in forest carbon storage in the Bantimurung Sub-Watershed during the 2014–2024 period. The estimation was carried out using the stock-difference approach, in which total carbon stock was calculated by integrating activity data, represented by forest cover area, with a site-specific forest carbon stock factor derived from field measurements. In this study, the average carbon stock value of 177.89 tons C ha^{-1} was used as the forest carbon stock factor for estimating carbon stock changes across the observation years.

The results showed that forest carbon stock increased from 302,710.08 tons C in 2014 to 329,703.10 tons C in 2019 and further increased to 332,618.72 tons C in 2024. Overall, forest carbon stock increased by 29,908.65 tons C during the 2014–2024 period. The largest increase occurred during the 2014–2019 period, with an increase of 26,993.03 tons C, while the 2019–2024 period showed a smaller increase of 2,915.62 tons C.

This increase was associated with the expansion of forest cover, particularly secondary dryland forest, and the sharp decline in open land during the observation period. Open land decreased from 123.56 ha in 2014 to 0.20 ha in 2024, while secondary dryland forest increased from 2.90 ha to 232.38 ha over the same period. These changes suggest that secondary forest regeneration contributed to the recovery of forest carbon stock in the Bantimurung karst landscape.

Table 7. Total soil carbon content

Site	Vegetation	Litter	Soil	Carbon value (Tons/Ha)
Site 1	83.89	8.80	16.00	108.69
Site 2	237.66	5.62	30.00	273.28
Site 3	117.24	9.46	25.00	151.70
Total				533.67
Average				177.89

Table 8. Dynamics of carbon stocks in the Bantimurung Sub-Watershed for the period 2014–2024

No.	Analysis Components	Year 2014	Year 2019	Year 2024	Change (2014–2024)
1	Forest area (Ha)	1701.67	1853.41	1869.8	+168.13
2	Total carbon stocks (Tons C)	302.710	329.703	332.619	29.909
3	Change status (Ton C)	—	26.993	2.916	—

The increase in forest carbon stock indicates that land cover transition toward more vegetated areas can support carbon accumulation over time. This finding is consistent with previous studies showing that forest regeneration and natural succession can increase biomass and carbon storage, particularly in landscapes where seed sources, remaining forest patches, and conservation areas support vegetation recovery (Yudono et al., 2022) (Fadhli, Sugianto, 2022)

However, the historical carbon stock estimates should be interpreted with caution. The carbon stock factor used in this analysis was derived from current field measurements, while vegetation structure and carbon density in 2014 and 2019 may have differed from the 2024 field condition. Therefore, the results are best understood as estimates of carbon stock change based on land cover dynamics and site-specific carbon stock values, rather than direct measurements of carbon stock in each historical year.

In this study, the analysis focused on forest cover classes, namely primary dryland forest and secondary dryland forest. This focus was applied to reduce overestimation because non-forest land cover classes, such as settlements, open land, rice fields, mixed dryland agriculture, and water bodies, generally have lower and more variable carbon stocks. Therefore, the reported carbon stock dynamics mainly represent the contribution of forest cover change and secondary forest regeneration to carbon recovery in the Bantimurung Sub-Watershed (Table 8).

In this study, the historical carbon stock analysis was focused only on forest cover classes by applying the conservativeness principle recommended in IPCC carbon accounting. This approach was used to avoid overestimation because non-forest land cover classes, such as rice fields, settlements, open land, mixed dryland agriculture, and water bodies, generally have lower and more variable carbon stocks than forest cover. In particular, seasonal agricultural land may have fluctuating carbon values due to planting and harvesting cycles.

Referring to the national (National Forest Reference Level for Deforestation, Forest Degradation and Enhancement of Forest Carbon Stock, 2022), carbon stock estimation for dynamic or seasonal land cover classes should be interpreted cautiously because their carbon density is strongly influenced by management practices and temporal variation. Therefore, this study used the average forest carbon stock value of 177.89 tons C ha^{-1} only as a site-specific carbon stock factor for forest cover classes, namely primary dryland forest and secondary dryland forest.

By focusing on forest cover, the carbon stock dynamics reported in this study represent the contribution of forest cover change and secondary forest regeneration to carbon recovery in the Bantimurung karst landscape. This approach provides a conservative estimate and reduces the possibility of overestimating carbon stocks from land cover classes with lower or less stable carbon storage capacity.

CONCLUSIONS

Based on the results of spatial analysis and field measurements in the Bantimurung Sub-Watershed, it can be Over the 2014–2024 period, the Bantimurung karst ecosystem experienced substantial land-cover transformation, marked by a dramatic decline in open land from 123.56 ha to only 0.20 ha and a simultaneous expansion of secondary dryland forest to 232.38 ha by 2024, indicating an active and ongoing forest regeneration process. This ecological recovery was accompanied by a high carbon storage capacity, with the ecosystem recording an average carbon stock of 177.89 tons C ha^{-1}, a value comparable to Indonesia's national average for primary dryland forests despite the challenging edaphic conditions of carbonate substrates and shallow soil profiles. Furthermore, a decade of natural succession combined with conservation interventions successfully increased total carbon stocks by 29.90 tons C, primarily driven by biomass accumulation

in regenerating secondary forest stands. These findings suggest that stricter monitoring of land-clearing activities in karst buffer zones is essential to protect the stability of SOC stocks, while future studies should integrate dissolved inorganic carbon measurements to better capture both biological and geochemical carbon dynamics in karst systems. In addition, the Tier 3-based carbon stock estimates generated in this study provide a robust technical foundation for developing regional carbon incentive mechanisms and payment for ecosystem services schemes.

REFERENCES

1. Bennett, N. J., Blythe, J., Cisneros-montemayor, A. M., Singh, G. G., Sumaila, U. R. (2020). *Just Transformations to Sustainability*, *6*, 1–18.
2. Chen, H., Fleskens, L., Baartman, J., Wang, F., Moolenaar, S., Ritsema, C. (2020). Science of the Total Environment Impacts of land use change and climatic effects on streamflow in the Chinese Loess Plateau : A meta-analysis. *Science of the Total Environment*, *703*, 134989. https://doi.org/10.1016/j.scitotenv.2019.134989
3. Curtis, P. G., Slay, C. M., Harris, N. L., Tyukavina, A., Hansen, M. C. (2018). Classifying drivers of global forest loss, *1111*(September), 1108–1111.
4. Danaë M.A. Rozendaal. (2022). Aboveground forest biomass varies across continents, ecological zones and successional stages: refined IPCC default values for tropical and subtropical forests. *Environmental Research Letters, 17*(1).
5. Donchyts, G., Winsemius, H., Baart, F., Dahm, R. (2022). High-resolution surface water dynamics in Earth's small and medium-sized reservoirs. *Scientific Reports*, 1–13. https://doi.org/10.1038/s41598-022-17074-6
6. Fadhli, Sugianto, S. (2022). Analisis perubahan penutupan lahan dan potensi karbon di Taman Hutan Raya Pocut Meurah Intan, Aceh Indonesia. January. *Jurnal Ilmu Lingkungan 19*(2):450–458. https://doi.org/10.14710/jil.19.2.450-458
7. Fajri, A., Hadi N.B., Indra A.S.L.P. Putri, Lestari, T. H., I Wayan, S. D., Hendalastuti, R. H., Sri, S., Ayun, W., Husnul, K., Tri, S., Supratman, T. (2024). Forest cover change and its carbon dynamic of the karst area in Bulusaraung, South Sulawesi, Indonesia. *Forest Science and Technology*, *20*(2), 179–193. https://doi.org/10.1080/21580103.2024.2343344
8. Forster, P. M., Smith, C., Walsh, T., Lamb, W. F., Lamboll, R. (2025). Indicators of Global Climate Change 2024: annual update of key indicators of the state of the climate system and human influence. *Earth System Science Data,* 2641–2680.
9. Friedlingstein, P., Sullivan, M. O., Jones, M. W., Andrew, R. M., Hauck, J. (2025). *Global Carbon Budget 2024*, 965–1039.
10. Fuady, S., Arsyad, M., Tiwow, V. A., Arsyad, F., Prasetiyo, A. (2025). Kuantifikasi cadangan karbon hutan kawasan karst Maros Taman Nasional Bantimurung Bulusaraung. *Jurnal Ilmu Lingkungan 23*(5), 1333–1342. https://doi.org/10.14710/jil.23.5.1333-1342
11. Gautam, M. K., Berg, B. (2025). Editorial: Plant litter decomposition: patterns, processes, and element cycling. February, 1–3. https://doi.org/10.3389/fenvs.2025.1562030
12. Guillaume, T., Kotowska, M. M., Hertel, D., Knohl, A., Krashevska, V., Murtilaksono, K., Scheu, S., Kuzyakov, Y. (2018). Conversion to plantations. *Nature Communications*, *9*, 2388. https://doi.org/10.1038/s41467-018-04755-y
13. Turner II, B.L., Lambin, E. F., Verburg, P. H. (2021). From land-use / land-cover to land system science. In: Ambio's 50th Anniversary Collection. Theme: Agricultural land use. *Ambio*, *50*(7), 1291–1294. https://doi.org/10.1007/s13280-021-01510-4
14. Krause, A., Pugh, T. A. M., Bayer, A. D., Lindeskog, M., Arneth, A. (2016). Impacts of land-use history on the recovery of ecosystems after agricultural abandonment. *Earth System Dynamics* 745–766. https://doi.org/10.5194/esd-7-745-2016
15. Liu, Y. S., Zhou, X., Yang, J. H., Hoepner, A. G. F., Kakabadse, N. (2023). Carbon emissions, carbon disclosure and organizational performance. *International Review of Financial Analysis*, *90*, 1–17. https://doi.org/10.1016/j.irfa.2023.102846
16. Meyfroidt, P., Bremond, A. De, Ryan, C. M., Archer, E., Aspinall, R., Erb, K. (2022). Ten facts about land systems for sustainability. *Proceedings of the National Academy of Sciences 119*(7), 1–12.
17. National forest reference level for deforestation, forest degradation and enhancement of forest carbon stock (2022).
18. Patterns, R. the I. of L. U. and L.-U. C. on M. R. and P., Wierik S. A., Cammeraat E. L. H., Gupta J., and Y. A. A.-R. (2021). Reviewing the impact of land use and land-use change on moisture recycling and precipitation patterns. *Water Resources Research*. https://doi.org/10.1029/2020WR029234
19. Peraturan Presiden Nomor 98 Tahun 2021 tentang Penyelenggaraan Nilai Ekonomi Karbon untuk Pencapaian Target Kontribusi yang Ditetapkan Secara Nasional dan Pengendalian Emisi Gas Rumah Kaca dalam Pembangunan Nasional. *Database Peraturan BPK*, *10*(1), 279–288.
20. Chazdon R.L, Lindenmayer D., Guariguata M.R, Crouzeilles R., Rey Benayas J.M., Chavero E.L.

(2020). Fostering natural forest regeneration on former agricultural land through economic and policy interventions. *Environmental Research Letters, 15*(4), https://doi.org/10.1088/1748-9326/ab79e6

21. Rosa, C. M. da, Marques, M. C. M. (2022). How are biodiversity and carbon stock recovered during tropical forest restoration? Supporting the ecological paradigms and political context involved. *Journal for Nature Conservation*, *65*, 126115. https://doi.org/https://doi.org/10.1016/j.jnc.2021.126115
22. Shamim, S., Zhen, L., Miah, G., Ahamed, T. (2020). Impact of land use change on ecosystem services: A review. *Environmental Development*, *34*(April), 100527. https://doi.org/10.1016/j.envdev.2020.100527
23. Shi, L., Zhao, Y., Zeng, S., Liu, Z., Shao, M., Zhao, M., He, H., Zeng, C., Han, Y., Hao, P., Tang, L. (2025). Land-use management and climate change can enhance the autotrophic capacity and reduce the CO_2 emissions of karst aquatic ecosystems. *Water Research*, *284*, 124031. https://doi.org/https://doi.org/10.1016/j.watres.2025.124031
24. Nasional S., Nasional, B. S. (2019). *Pengukuran dan penghitungan cadangan karbon – Pengukuran lapangan untuk penaksiran cadangan karbon berbasis lahan*. Standar Nasional Indonesia.
25. Valencia, S., Camilo, J., Hoyos, N., Duque-Villegas, M., Salazar, J. F. (2024). Regional studies streamflow response to land use / land cover change in the tropical Andes using multiple SWAT model variants. *Journal of Hydrology: Regional Studies*, *54*(July), 101888. https://doi.org/10.1016/j.ejrh.2024.101888
26. Wu, Q., Ni, X., Sun, X., Chen, Z., Hong, S. (2025). Substrate and climate determine terrestrial litter decomposition. *PNAS*, 1–8. https://doi.org/10.1073/pnas
27. Yudono, H., Hadi, S., Nurfatriani, F., Indrajaya, Y., Yuwati, T. W., Allo, M. K., Muin, N., Isnan, W., Ardie, I., Liannawatty, S., Putri, P., et al. (2022). Mainstreaming ecosystem services from Indonesia' s remaining forests. *Sustainability*, 14(19), 12124; https://doi.org/10.3390/su141912124
28. Zhang, J., Liesch, T., Chen, Z., Goldscheider, N. (2023). Global analysis of land-use changes in karst areas and the implications for water resources. *Hydrogeology Journal, 31*, 1197–1208. https://doi.org/10.1007/s10040-023-02650-5
29. Zhou, Q., Luo, A.-Y., Shi, A.-C. (2023). Hydrological effects of vegetation restoration in karst areas research: Progress and challenges. *Transactions in Earth Environment and Sustainability, 1*(2-3), https://doi.org/10.1177/2754124X231199565